Comet Giacobini-Zinner: In Situ Observations of Energetic Heavy Ions

F. M. Ipavich, A. B. Galvin, G. Gloeckler, D. Hovestadt, B. Klecker, M. Scholer

Conclusive evidence is presented for the existence of energetic (~35,000 to 150,000 electron volts), heavy (≳12 atomic mass units), singly charged cometary ions within ~1.5 × 10^6 kilometers of comet Giacobini-Zinner. The observations were made with the University of Maryland/Max-Planck-Institut ultralow-energy charge analyzer on the International Cometary Explorer spacecraft. The most direct evidence for establishing the mass of these ions was obtained from an analysis of the energy signals in one of the solid-state detectors; it is significant at the three-sigma level. Maximum fluxes were recorded ~1 hour before and ~1 hour after closest approach to the cometary nucleus. Transformation of the particle angular distributions observed at ~50,000 kilometers radial distance from the comet during the inbound pass into a rest frame in which the distributions are nearly isotropic requires a transformation velocity that is consistent with the local solar wind velocity if one assumes that these particles are primarily singly ionized with a mass of 18 ± 6 atomic mass units. The existence of a frame of reference in which these water-group ions were isotropic implies that they underwent strong pitch angle scattering after their ionization. Particle energies in the rest frame extend to substantially higher values than would be expected if these ions were locally ionized and then picked up by the solar wind, implying that the ions were accelerated or heated. The derived ion density, ~0.1 per cubic centimeter, is consistent with a crude model for the production and transport of pickup ions.

One of the outstanding problems of cometary physics is the interaction of the cometary gas with the solar wind. Biermann *et al.* (*1*) first suggested that momentum transfer between solar wind and cometary material is due to the collisionless interaction of ionized cometary gas and the interplanetary magnetic field. Because of the extremely low gravity of the cometary body, neutral molecules and atoms evaporated from the surface can escape freely into space from the collision-dominated inner region of the comet with a velocity generally assumed to be ~1 km sec^{-1}. These molecules are subjected to complicated chemical reactions in the inner coma and, farther out, to a variety of photodissociative and ionizing processes (*2*). As a result, a few types of parent molecules, such as H_2O, CO_2, NH_3, CH_4, and CO, of direct cometary origin, produce a variety of molecular and atomic ions. Spectroscopically identified ions include OH^+, H_2O^+, C^+, CO^+, CO_2^+, CH^+, CN^+, N_2^+, H_2S^+, and Ca^+ (*3*). The source density of these ions is determined by the gas production rate and the cross sections for dissociation and ionization.

Freshly ionized particles in the solar wind are subject to the combined forces of the interplanetary electric $\mathbf{v}_{sw} \times \mathbf{B}$ field (where $\mathbf{v}_{sw}$ is the solar wind velocity and $\mathbf{B}$ is the interplanetary magnetic field) and the magnetic field frozen into the solar wind, as well as to a variety of wave-particle interactions. In the region well upstream of the comet, where magnetic fluctuations are small, the ions initially perform cycloidal motions. The pitch angle distribution of these particles in the solar wind frame is a ring in velocity space with pitch angle π-α, where α is the angle between the solar wind velocity and the local magnetic field. In the presence of strong pitch angle scattering, the distribution function in the solar wind frame will become a spherical shell with a speed equal to the solar wind speed. This type of pickup process has recently been identified for the case of singly ionized helium of interstellar origin, which is ionized by solar ultraviolet radiation, picked up by the frozen-in interplanetary magnetic field, and then adiabatically decelerated in the expanding solar wind (*4*).

The International Cometary Explorer (ICE) mission to comet Giacobini-Zinner provided the first in situ measurements of freshly ionized cometary particles and of their dynamics. On 11 September 1985 the ICE spacecraft traversed the cometary tail downstream from the nucleus at a distance of 7800 km at closest approach. We report here the first results obtained with the ultra-low-energy charge analyzer (ULECA) of the University of Maryland/Max-Planck-Institut (*5*) on ICE.

Instrumentation. The ULECA sensor, which was designed to measure H^+, He^{2+}, and highly ionized heavy particles, consists of an electrostatic deflection system and an array of solid-state detectors that allow the determination of an ion's charge state from the simultaneous measurement of energy per charge and total energy. Detectors M1, M2, and M3 have mean energy-per-charge responses of ~33, 66, and 130 keV e^{-1} for protons and multiply charged ions. For singly ionized heavy ions the mean energies are ~35, 70, and 150 keV e^{-1}. The energy resolutions ($\Delta E/E$, full width at half maximum) are ~20, 27, and 37 percent, respectively, for the three detectors. Detector L2 has a lower energy response (10 to 30 keV e^{-1}), but has a complicated mass-dependent efficiency. The ULECA sensor samples particles in the ecliptic plane in eight 45° sectors, with an acceptance angle ±30° out of the ecliptic plane; no information is available on the angular distributions perpendicular to the ecliptic plane. One of the sectors is centered on the solar direction. Each M detector has three rates, determined by appropriate energy windows, generally responding to particles with ionic charge state $Q = 1$, $Q = 2$, and $Q \geq 3$. ULECA is completely insensitive to neutral and negatively charged particles.

Although the instrument was not designed to measure heavy molecules with low charge states such as cometary ions, the ULECA sensor is sensitive to these ions during periods of sufficiently high fluxes. While the electrostatic deflection system provides a cleanly defined energy-per-charge passband, the detection efficiency of heavy particles in the solid-state detectors is not determined as precisely. The response of the ULECA sensor to singly charged heavy ions (*6*) is described here.

Since all ions striking a given solid-state detector have the same energy per charge, one would expect the energy recorded by the solid-state detector to be proportional to the charge state of the ion. This is not the case, however, because of "pulse height defect" that results from the occurrence of nonionizing (and hence unmeasured) energy losses in the detector (*7*). This effect causes a heavy ion to produce a smaller energy signal than a lighter ion with the same incident energy. For example, in detector M3, H^+ ions produce a mean energy signal of ~95 keV, He^+ produces ~80 keV, and O^+ produces ~30 keV. With the electronic discriminator set at ~62 keV for detector M3, one would not expect this detector to respond to an O^+ ion. However, the statistical nature of pulse height defect combined with noise in the detector and

F. M. Ipavich, A. B. Galvin, G. Gloeckler, Department of Physics and Astronomy, University of Maryland, College Park, MD 20742.
D. Hovestadt, B. Klecker, M. Scholer, Max-Planck-Institut für Extraterrestrische Physik, 8046 Garching, West Germany.

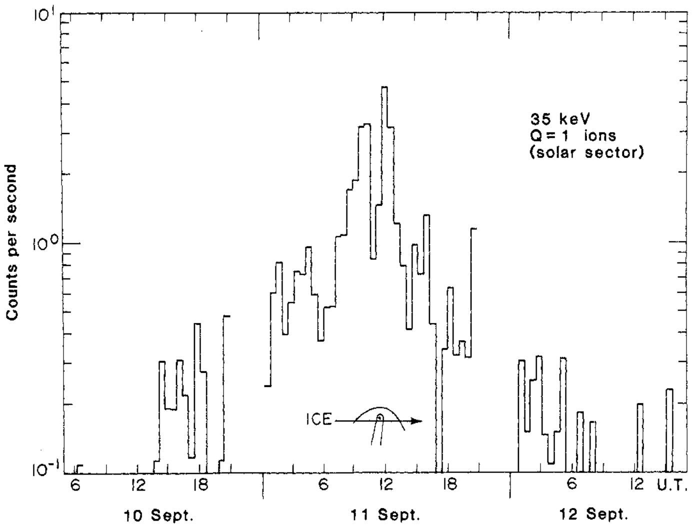

Fig. 1. Background-corrected counting rate profile of detector M1 (34-minute averages). The inset at the bottom shows the cometary boundaries to scale.

associated electronics results in a nonzero efficiency for the singly charged heavy ion response. On the basis of preflight and in-flight detector calibrations, we have determined the efficiencies for each of the M detectors. For H_2O^+ ions this efficiency varies from 0.01 to 0.03 for the three detectors. The CO^+ efficiencies are $\sim 10^{-3}$ and the CO_2^+ efficiencies are less than 10^{-4}. The efficiencies are sensitive to a number of effects; we estimate that the overall uncertainty in the absolute efficiencies is approximately a factor of 2.

Temporal behavior of particle intensities. Throughout the encounter the maximum flux is generally observed in the sun-viewing sector. Figure 1 displays the counting rate profile (34-minute averages) of this sector for the M1 detector (~35-keV singly charged ions) for a 60-hour period centered on the comet traversal. (The detector background counting rate of 2.6 counts per second has been subtracted; the one-sigma counting statistics error is 0.1 count per second.) The inset near the bottom of Fig. 1 represents an approximately scaled drawing of the Giacobini-Zinner cometary bow wave and tail regions. The first significant counting rate observed by this detector occurred somewhat before 1500 universal time (U.T.) on 10 September, when the ICE spacecraft was located $\sim 1.5 \times 10^6$ km from the cometary nucleus. The highest counting rates were observed on either side of the cometary tail. The counting rate values in Fig. 1 may be converted to differential intensities (ions per square centimeter per second per steradian per kiloelectron volt) by multiplying by ~5000 if the ions are from the water group.

Figure 2 shows 512-second averaged counting rate profiles of the three energy channels M1, M2, and M3, as recorded in the solar sector. On the inbound approach the lowest energy channel reached a maximum of ~7.5 counts per second at ~1010 U.T. and then dropped nearly to background levels for ~30 minutes centered on the cometary tail. On the outbound pass the maximum rate of ~10 counts per second was reached at about 1225 U.T. Several less-sustained rate increases were seen thereafter. The medium energy channel M2 showed a somewhat different behavior, displaying a broad maximum seen at least 30 minutes before the M1 peak rate. The rate depression in the tail region also lasted longer than that for M1. The highest energy channel, M3,

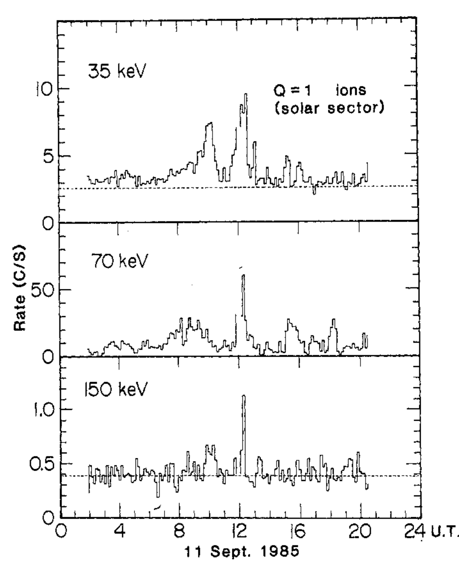

Fig. 2. Counting rate profiles (512-second averages) of detectors M1 (top panel), M2 (center panel), and M3 (bottom panel) from the solar viewing sector. The mean energy responses indicated are approximate and depend somewhat on the mass of the ions. The background rates for M1 and M3 are shown by dashed lines. The background rate for M2 is variable and has already been subtracted.

showed significant rate increases only near the times of the M1 maximum rates.

Mass identification. Identification of the mass of the ions producing the observed response requires analysis of the energy pulse height data. As described above, singly ionized particles with different masses produce different energy signals, allowing the separation of, for example, H^+ from H_2O^+. The energy signals from the singly charged heavy particles are strongly peaked near the electronic threshold for each of the three detectors, while the energy deposited by H^+ is somewhat higher. In the M1 and M2 detectors the H^+ measured energy is too close to the threshold to allow easy separation from heavier ions. In the M3 detector, however, such a separation is possible. Table 1 summarizes our analysis of the energy signals in the M3 detector for the combined time periods 0950 to 1030 U.T. and 1200 to 1235 U.T. on 11 September 1985; these periods were adjacent to the cometary tail region.

Essentially all the energies produced by water-group ions (O^+, OH^+, H_2O^+, and H_3O^+) are expected to fall in the channel number range 15 to 20 (channel 15 is the threshold for detector M3). This range will also contain lighter ions, such as C^+ and N^+. Heavier particles such as CO^+ and CO_2^+ will also fall into this range but have a much smaller probability of being detected; their efficiency is 10 to 100 times lower than that of H_2O^+. The second channel number range would contain ~90 percent of H^+ energy counts (O^{2+} and H_2^+ ions would also fall in the second range). The third channel number range should not contain any ions that are expected to be present in the cometary environment.

Table 1 lists the observed number of counts and also the expected number of background counts in each of the three channel number ranges. Background values were derived by using the standard technique (*6*) of normalizing a quiet-time pulse height spectrum with the ratio of quiet-time to active-time counting rates. The final column of Table 1 lists the ratio of the net counting rate to the one-sigma error. The range containing the water-group ions is significant at the three-sigma level while the other ranges are not statistically different from the expected background. We conclude that the M3 detector is responding primarily to singly ionized particles with a mass of $\gtrsim 12$ amu.

Distribution functions. We analyzed the angular distributions of the counting rates in each of the three rate channels by transforming the distribution function $f(v)$ using the technique described by Gloeckler *et al.* (*8*) (which was successfully applied to stud-

Table 1. Identification of measured ions in detector M3 (113 to 158 keV e^{-1} incident energy per charge) for the combined time periods 0950 to 1030 U.T. and 1200 to 1235 U.T.

Energy channel range	Expected dominant ion	Counts			Net σ
		Observed	Background	Net	
15 to 20	Water group	44	16.8	27.2 ± 7.8	3.5
21 to 31	H^+	29	21.4	7.6 ± 7.1	1.1
32 to 41	Background	6	10.6	−4.6 ± 4.1	−1.1

ies of convective flows in the geomagnetic tail). It was assumed (and subsequently verified for the time interval presented here) that $f(v)$ was isotropic in some reference frame. Using an initial estimate of the velocity of this rest frame with respect to the spacecraft frame, we mapped the differential intensity derived from each statistically significant sectored counting rate at the center look direction of each 45° angular sector into three segments of the distribution function corresponding to the three energy channels. The magnitude and direction of the velocity of the rest frame were varied by an iterative procedure until all segments of the distribution function lined up to form a smooth spectrum; if it were not possible to produce a smooth spectrum, then the distribution function would not have been isotropic in any rest frame. This method of analysis requires no prior knowledge of the spectral shape, nor need the speed of the rest frame be much less than the particle speed.

We applied this technique to the time interval 0959 to 1030 U.T., some 45 minutes and 50,000 km before closest approach. The result is shown in Fig. 3, which displays the distribution function $f(v)$ versus particle speed in the rest frame. The derived rest frame speed, as well as particle speed, is inversely proportional to the square root of the mass-to-charge ratio of the ions. If we assume that these ions were singly ionized with mass 18, as is done in Fig. 3, then the derived rest frame speed is 230 km sec^{-1}, a value compatible with the (variable) solar wind speed averaged over the same time interval (*9*). If, however, we assume that all the ions were protons, then the derived rest frame speed is ~1000 km sec^{-1}, a value greatly exceeding the measured solar wind speed. We conclude that the instrument was responding primarily to ions in the mass range 18 ± 6 amu, consistent with the direct measurement presented above, and that these ions were isotropic in a rest frame moving with approximately the solar wind speed.

For completeness, we mention that the ultralow-energy wide-angle telescope (ULEWAT) sensor of the experiment, although sensitive to energetic electrons, recorded no increase during the cometary traversal. The upper limits for the differential intensity (electrons per square centimeter per second per steradian per kiloelectron volt) are $\sim 10^{-2}$ at 100 keV and $\sim 5 \times 10^{-4}$ at 200 keV.

Discussion. We observed singly ionized heavy cometary particles at energies up to ~150 keV. Analysis of the energy signals of the solid-state detector responding to the highest incident energies indicates that the ion mass was ≳12 amu. In view of the decreasing efficiency of the detector for increasingly heavy ions and the expected ion abundances in the cometary environment (*2*, *3*), one would expect that these ions are primarily from the water group.

This identification is independently supported by analysis of the observed angular distributions over our entire energy range, which become isotropic when transformed with approximately the local solar wind speed only if the mass per charge of these ions is ~18 ± 6. We emphasize that the angular distributions analyzed here were observed in the turbulent region some 50,000 km from the cometary nucleus. At larger distances (>10^5 km), Hynds *et al.* (*10*) reported angular distributions that are not consistent with isotropy in the solar wind frame. Our derived rest frame distribution function, displayed in Fig. 3, leads to two conclusions:

1) That there exists a rest frame in which the ions are isotropic implies that they have undergone strong pitch angle scattering, since their initial pitch angle distribution after ionization is highly anisotropic in the solar wind frame.

2) The ions were initially ionized in a region where the solar wind speed was substantially higher than that observed at the spacecraft location. If these pickup ions had been locally ionized and pitch angle–scattered without energy change, they would have had a sharp cutoff at the local solar wind speed of ~230 km sec^{-1} (arrow in Fig. 3). Such a cutoff has been observed for the case of freshly ionized interstellar helium (*4*). The substantially higher speeds (~1000 km sec^{-1}) observed in the present case are clearly at variance with this expectation unless an unreasonably large energy increase (factor of ~20) is postulated. We conclude that these ions were originally created far upstream from the comet in a region where the solar wind speed is ~500 km sec^{-1} (*9*) and then accelerated or heated during their transport to the spacecraft location.

There are several possible explanations for the observed large particle speeds in the rest frame. Fermi acceleration (*11*) or collective wave-particle interactions (*12*) may be important in the cometary upstream region. Another explanation relies on the possibility that the pickup ions do not become fully thermalized into the solar wind. Rather, ions produced in the far-upstream region suffer little pitch angle scattering and form a ring distribution in velocity space with a pitch angle determined primarily by the interplanetary magnetic field direction and a speed in the solar wind frame of ~500 km sec^{-1} [the preencounter solar wind speed (*9*)]. The ions undergo increased pitch angle scattering and eventually become isotropic in the solar wind frame as they are convected by the magnetic field embedded in the solar wind into the near-cometary environment characterized by increased turbulence and larger ion production rates. The mass loading slows the solar wind and compresses the magnetic field. Compression of the magnetic field by a factor of 2 to 3 (*13*) from the far-upstream region to the location of our measurements would produce an increase in the perpendicular particle energy by the same factor if the magnetic moment

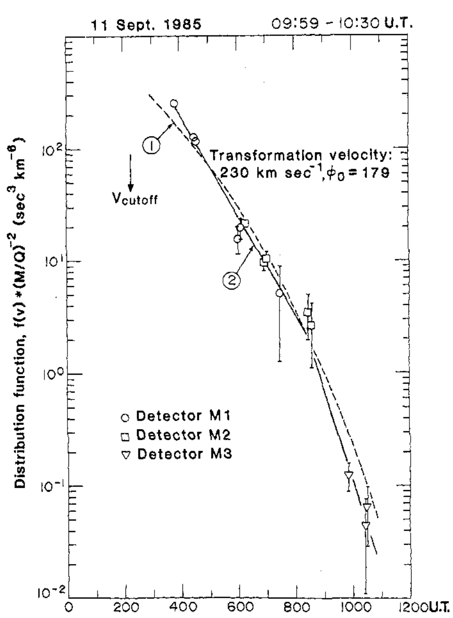

Fig. 3. Distribution function derived by the method described in the text. The computed transformation velocity is approximately equal to the local solar wind speed. Curves 1 and 2 are described in the text.

($\propto v_\perp^2/B$) were conserved. A maximum particle speed of ~800 km sec^{-1} would then result, a value somewhat less than that observed (Fig. 3).

In this scenario, one would expect relatively few particles with the maximum speed, since most of the ions are produced near the comet in a region where the solar wind speed is less than it is far upstream and where the magnetic field is already enhanced. Qualitatively, one thus expects a spectrum decreasing with increasing velocity, as is observed (Fig. 3). A quantitative assessment would require knowledge of both the solar wind velocity and the cometary ion density as functions of position. The sharp cutoff at some maximum speed expected in this model is not observed. However, the highly turbulent magnetic field and solar wind behavior (*9, 13*) at the location of our measurements would broaden the expected cutoff, as would the presence of multiple ion species. Ogilvie *et al.* (*14*) analyzed the ion composition at much lower energies and reported substantial densities of ions heavier than those of the water group. If all the cometary ions have the same maximum speed, ~800 km sec^{-1}, then detector M3 (triangles in Fig. 3) might in fact be responding to CO^+ ions, even though the detector efficiency for CO^+ is much lower than for water-group ions. Recall that the velocity axis in Fig. 3 scales as the square root of the mass per charge of the ions being detected. CO^+ ions with a speed of 800 km sec^{-1} would correspond to a water ion speed of ~1000 km sec^{-1} in Fig. 3.

Yet another explanation of the observed high particle speeds is that the ions have been thermalized and heated in the region where the solar wind slows. We have fit a Maxwellian [$f \propto \exp(-E/kT)$, curve 1 in Fig. 3] to the rest-frame distribution function over our observed range of ~380 to 1050 km sec^{-1}. The resulting Maxwellian is characterized by a density of 0.05 ion cm^{-3} and an e-folding energy of $kT = 11$ keV, corresponding to a thermal speed $(kT/M)^{1/2}$ of 240 km sec^{-1}. This value for the thermal speed is in reasonable agreement with the results of single-component stationary hydrodynamic calculations that postulate the complete thermalization of new cometary ions after they are picked up by the solar wind (*15, 16*), if one assumes that the thermalization has equalized the thermal speeds rather than the temperatures of solar wind and cometary ions.

The moments of the observed distribution function may, alternatively, be evaluated by approximating the distribution function by the two line segments constituting curve 2 in Fig. 3. Extrapolating this representation to zero speed results in a calculated density of 0.1 cm^{-3} and mean energy of 9 keV, values similar to those derived under the assumption of a Maxwellian distribution. The computed energy densities for the two assumed forms of the distribution function are 800 and 900 eV cm^{-3}. This rest frame energy density is comparable to that in the simultaneously measured magnetic field. During the measurement time of the spectrum in Fig. 3, the magnetic field varied from ~8 to 22 nT (*13*), corresponding to energy densities of ~160 to 1200 eV cm^{-3}.

Finally, we compare our observed densities with the predictions of a simple model of the pickup process for water-group ions. The production rate P of ions per cubic centimeter per second is given by (*15*)

$$P = \frac{Q}{4\pi\tau v_N R^2} \exp\left(-\frac{R}{\tau v_N}\right) \qquad (1)$$

where $Q \simeq 3.5 \times 10^{28}$ sec^{-1} is the number of neutral water molecules released from the comet per second (*17*), $v_N \simeq 1$ km sec^{-1} is the radial speed of the neutral molecules, R is the distance from the nucleus, and τ is the ionization time.

The ionization time is somewhat difficult to estimate. Two ionization processes that are certainly operative are

1) Photolytic reactions. If one considers only the neutral parent molecule H_2O and only the destruction processes of photodissociation and photoionization, then the reaction rates (*2*) imply that the steady state consists of 97 percent O^+ and 3 percent H_2O^+ with an effective ionization time of 5×10^6 seconds.

2) Charge exchange between cometary neutrals and solar wind protons. Typical cross sections for this process are in the range 1×10^{-15} cm^2 to 3×10^{-15} cm^2 (*18, 19*). The measured (*9*) solar wind density (~5 cm^{-3}) and speed (~500 km sec^{-1}) shortly before entering the strong cometary interaction region then produce a characteristic ionization time of ~2×10^6 seconds.

Many other ionization processes, some of them spatially inhomogeneous, have been postulated (*3*). Chemical reactions (*2*) are also important in determining the evolution of cometary ion abundances. For our purposes we adopt $\tau = 10^6$ seconds (*15*), recognizing the uncertainty in this value.

The newly created water-group ions are then picked up by the solar wind and convected downstream toward the spacecraft location. The flux F of these ions is given by

$$F = \int_{x_0}^{\infty} P\,dx \qquad (2)$$

resulting in a density $n_I = F/v_{sw}$, where v_{sw} is the local solar wind speed. In the presence of strong pitch angle scattering, the ions quickly become isotropic in the solar wind frame so that the integral should be evaluated over the path of a solar wind plasma element and should take into account the deflection of the solar wind caused by the presence of the comet. Here we ignore this effect and approximate the actual ICE encounter geometry (*17*) with an orthogonal coordinate system centered on the cometary nucleus, the x-axis directed toward the sun and the z-axis parallel to the ICE trajectory. In this system the ICE trajectory is characterized by $x = x_0 = -8000$ km and the ICE location at the time of the Fig. 3 spectrum is $x = -8000$ km and $z = -50{,}000$ km. Inserting Eq. 1 into Eq. 2, noting that $R^2 = x^2 + z^2$, and taking $v_{sw} = 230$ km sec^{-1} (our measured rest frame speed), we find for the spacecraft location at the measurement time a predicted density $n_I = 0.4$ cm^{-3}, in reasonable agreement with our measured value ($n_I = 0.05$ to 0.1 cm^{-3}), given the uncertainties in both the model calculation and the observations.

REFERENCES AND NOTES

1. L. Biermann, B. Brosowski, H. U. Schmidt, *Sol. Phys.* **1**, 254 (1967).
2. W. F. Huebner and P. T. Giguere, *Astrophys. J.* **238**, 753 (1980).
3. D. A. Mendis, H. L. F. Houpis, M. L. Marconi, *Fundam. Cosmic Phys.* **10**, 1 (1985).
4. E. Mobius *et al.*, *Nature (London)* **318**, 426 (1985).
5. D. Hovestadt *et al.*, *IEEE Trans. Geosci. Electron.* **GE-16**, 166 (1978).
6. F. M. Ipavich *et al.*, *Geophys. Res. Lett.* **11**, 504 (1984).
7. F. M. Ipavich, R. A. Lundgren, B. A. Lambird, G. Gloeckler, *Nucl. Instrum. Methods* **154**, 291 (1978).
8. G. Gloeckler *et al.*, *Geophys. Res. Lett.* **11**, 603 (1984).
9. S. J. Bame *et al.*, *Science* **232**, 356 (1986).
10. R. J. Hynds *et al.*, *ibid.*, p. 361.
11. E. Amata and V. Formisano, *Planet. Space Sci.* **33**, 1243 (1985).
12. K. Papadopoulos and J. D. Huba, unpublished manuscript.
13. E. J. Smith *et al.*, *Science* **232**, 382 (1986).
14. K. W. Ogilvie *et al.*, *ibid.*, p. 374.
15. H. U. Schmidt and R. Wegmann, in *Comets*, L. L. Wilkening, Ed. (Univ. of Arizona Press, Tucson, 1982), p. 538.
16. W.-H. Ip and W. I. Axford, *ibid.*, p. 588.
17. T. T. von Rosenvinge, J. C. Brandt, R. W. Farquhar, *Science* **232**, 353 (1986).
18. L. Biermann and R. Lust, in *The Solar System*, B. Middlehurst and G. P. Kuiper, Eds. (Univ. of Chicago Press, Chicago, 1963), vol. 4, chap. 18.
19. D. A. Mendis, T. E. Holzer, W. I. Axford, *Astrophys. Space Sci.* **15**, 313 (1972).

20. We thank the many individuals at the University of Maryland and the Max Planck Institute for Extraterrestrial Physics for their contributions to this experiment, especially E. Tums, J. Cain, P. Laeverenz, and E. Kunneth. We also thank our co-investigators C. Y. Fan, L. A. Fisk, and J. J. O'Gallagher for their contributions and the other ICE experimenters for exchanging their data before publication. We have benefited from stimulating conversations with M. A'Hearn and M. Lee. We congratulate the ISEE/ICE project office and the many other individuals (particularly R. Farquhar) and institutions involved in making the ICE encounter with comet Giacobini-Zinner such an outstanding success. Supported by NASA under contract NAS5-28704 and grants NAGW101 and NGR 21-002-316 and by the Bundesministerium für Forschung und Technologie, Federal Republic of Germany, under contract RV14-B8/74.

20 November 1985; accepted 11 February 1986